

Catalytic ozonation of organic compounds in water over the catalyst of $\text{RuO}_2/\text{ZrO}_2\text{-CeO}_2$

Jianbing WANG (✉)¹, Guoqing WANG¹, Chunli YANG¹, Shaoxia YANG², Qing HUANG¹

¹ School of Chemical and Environmental Engineering, Beijing Campus, China University of Mining and Technology, Beijing 100083, China

² School of Energy and Power Engineering, North China Electric Power University, Beijing 102206, China

© Higher Education Press and Springer-Verlag Berlin Heidelberg 2014

Abstract This research investigates the performances of $\text{RuO}_2/\text{ZrO}_2\text{-CeO}_2$ in catalytic ozonation for water treatment. The results show that $\text{RuO}_2/\text{ZrO}_2\text{-CeO}_2$ was active for the catalytic ozonation of oxalic acid and possessed higher stability than $\text{RuO}_2/\text{Al}_2\text{O}_3$ and Ru/AC . In the catalytic ozonation of dimethyl phthalate (DMP), $\text{RuO}_2/\text{ZrO}_2\text{-CeO}_2$ did not enhance the DMP degradation rate but significantly improved the total organic carbon (TOC) removal rate. The TOC removal in catalytic ozonation was 56% more than that in noncatalytic ozonation. However this does not mean the catalyst was very active because the contribution of catalysis to the overall TOC removal was only 30%. The adsorption of the intermediates on $\text{RuO}_2/\text{ZrO}_2\text{-CeO}_2$ played an important role on the overall TOC removal while the adsorption of DMP on it was negligible. This adsorption difference was due to their different ozonation rates. In the catalytic ozonation of disinfection byproduct precursors with $\text{RuO}_2/\text{ZrO}_2\text{-CeO}_2$, the reductions of the haloacetic acid and trihalomethane formation potentials (HAAFPs and THMFPs) for the natural water samples were 38%–57% and 50%–64%, respectively. The catalyst significantly promoted the reduction of HAAFPs but insignificantly improved the reduction of THMFPs as ozone reacts fast with the THMs precursors. These results illustrate the good promise of $\text{RuO}_2/\text{ZrO}_2\text{-CeO}_2$ in catalytic ozonation for water treatment.

Keywords ozonation, ruthenium, oxalic acid, dimethyl phthalate, disinfection byproduct

1 Introduction

Endocrine disruptors (ECDs) and disinfection byproducts (DBPs) have become of great concerns as emerging contaminants due to their adverse biological effects [1,2]. Dimethyl phthalate (DMP), a typical endocrine disruptor, was frequently identified in Chinese surface water samples [1,3]. Haloacetic acids (HAAs) and Trihalomethanes (THMs), two kinds of typical DBPs, were also identified in Chinese drinking water samples. It was reported that the concentrations of HAAs in the drinking water samples from the water treatment plants in North China were about $25\text{--}30\ \mu\text{g}\cdot\text{L}^{-1}$ [4,5], and a one-year-long monitoring project conducted in a water treatment plant in North China showed that the highest concentration of THMs was $500\ \mu\text{g}\cdot\text{L}^{-1}$ [6].

Conventional water treatment processes can not completely remove ECDs and DBP precursors from water [2]. In contrast, heterogeneous catalytic ozonation is a promising technology for efficient removal of them from water. It combines ozone with adsorptive and oxidative solid phase catalysts to achieve high degradation and mineralization rate of organic compounds [2,7,8]. The key to the development of heterogeneous catalytic ozonation is the use of active and stable catalysts. In the last decades metals or metal oxides deposited on porous materials (e.g., alumina and activated carbon) were widely proposed in this field [9–14]. Ruthenium catalysts supported on alumina and activated carbon were found to be active in the catalytic ozonation for the treatment of dimethyl phthalate in water [13,14]. However, both alumina and activated carbon have some drawbacks. Alumina was likely leached into aqueous solution from the catalysts, and activated carbon was easily oxidized by ozone, both of which would result in the gradual reduction of catalyst activity for long time use [13–15].

In our previous study, zirconium-cerium mixed oxide

(ZrO₂-CeO₂) was found to be stable in catalytic wet air oxidation under high temperature and pressure conditions [16–18]. Higher stability of ZrO₂-CeO₂ is speculated in catalytic ozonation under room temperature condition. Both catalytic wet air oxidation and catalytic ozonation involve the same mechanism that the recalcitrant organic compounds are mainly removed by the oxidation of hydroxyl radicals. It was also widely proposed that the addition of catalyst into these two reaction systems can significantly enhance the production of hydroxyl radicals [17–19]. As RuO₂/ZrO₂-CeO₂ was reported to be active in catalytic wet air oxidation [16], it might also be active in catalytic ozonation. To the best of our knowledge the performance of RuO₂/ZrO₂-CeO₂ in catalytic ozonation has never been reported. Thus it is interesting to investigate the use of RuO₂/ZrO₂-CeO₂ in catalytic ozonation for water treatment.

In this work, RuO₂/ZrO₂-CeO₂ was prepared and its performance in catalytic ozonation was studied. The potential of RuO₂/ZrO₂-CeO₂ catalyzed ozonation for water treatment was explored with oxalic acid aqueous solution, DMP aqueous solution and natural water samples, respectively. Oxalic acid was selected as a model pollutant to study RuO₂/ZrO₂-CeO₂ catalyzed ozonation because of its ineffective removal in noncatalytic ozonation [10].

2 Materials and methods

2.1 Materials

2.1.1 Chemicals and reagents

Oxalic acid (99.999% pure) was purchased from Sigma-Aldrich (Saint Louis, USA). DMP (A.R.) was purchased from Tianjin Chemical Reagent No.1 Plant (China). A commercial hypochlorite sodium solution was used for chlorination and chlorine dioxide was prepared in the laboratory. Esterification reagent, methyl tertiary-butyl ether (MTBE), acetone and methanol with high purity grade were all obtained from Dima Tech. Co. (Nanjing, China).

Four THMs standards, chloroform (CHCl₃), bromodichloromethane (CHCl₂Br), dibromochloromethane (CHClBr₂) and bromoform (CHBr₃), one internal standard (Bromofluorobenzene) and surrogate compound (decafluorobiphenyl) (all > 99% pure) were obtained from Sigma-Aldrich Co. (Saint Louis, USA).

Six HAAs standards, monochloroacetic acid (MCAA), monobromoacetic acid (MBAA), dichloroacetic acid (DCAA), trichloroacetic acid (TCAA), bromochloroacetic acid (BCAA) and bromodichloroacetic acid (BDCAA),

one internal standard (1,2,3-trichloropropane) and surrogate compound (2,3-dibromopropionic Acid) (all > 99% pure) were purchased from Chem. Service, Inc. (West Chester, USA).

2.1.2 Sampling information

Natural water samples were withdrawn from eleven sites of the Chinese Jingmi Cannel, a source of drinking water for Beijing (Fig. S1). The sampling sites were Qiaoxin Town, Beishicao Town, Xingshou Town, Nanshao Town, Machi Kou, Yangfan Town, Hotspring Town, Blue-dragon Bridge, Huoqiying Bridge, Changchun Bridge, and Yuyuan Pond, respectively. Each sites had 7 samples. The water samples were pretreated by the filtration with 0.45 μm membrane to remove algae, bacteria and suspended particles.

2.1.3 Preparation of RuO₂/ZrO₂-CeO₂

The catalyst of RuO₂/ZrO₂-CeO₂ was prepared with wetness impregnation method followed by the thermal processing of microwave irradiation. Aqueous solution containing 0.9 mol·L⁻¹ Ce(NO₃)₃ and 0.1 mol·L⁻¹ ZrOCl₂ were added dropwise into ammonia aqueous solution under vigorous stirring. After precipitation the mixtures were filtered. The precipitate was then dried at 100°C for 24 h and calcined at 600°C for 5 h. The resultant powder composed of zirconium and cerium mixed oxides was used as the support for catalyst preparation. The support was then immersed in 6 mL RuCl₃ solution for 36 h at room temperature. After drying at 100°C for 12 h, the mixture was uniformly filled in a quartz reactor which was put inside a microwave oven (Sanyo, EM-202MS1, China) and then irradiated for 5 min at the power of 300 W. When the catalyst was irradiated, the temperature rising course of the catalyst bed was recorded using an Inconel sheltered type-K thermocouple probe (Beijing Wisdom Prosper Technologies Co., Ltd., China). The resultant catalyst presented a state of powder with ruthenium on the surface and was labeled as RuO₂/ZrO₂-CeO₂. The measured pH_{pzc} for it was 6.0. During the microwave irradiation some powder catalysts are easy to agglomerate and they were pulverized into the powder with particle size less than 4 μm before use in semi-batch reactor.

As the powder catalyst cannot be used in dynamic reactor, we also developed pelletized catalyst of RuO₂/ZrO₂-CeO₂. To prepare the pelletized catalyst, the powder ZrO₂-CeO₂ supports were developed into about 2 mm pellets by the methods described in our previous work [16]. The supports were then impregnated into RuCl₃ solution followed by microwave irradiation as described above. Unless otherwise specifically stated, the nominal ruthenium loading for all the catalysts was 0.5 wt.%.

2.2 Oxidation reactions

2.2.1 Semi-batch experiments

Stripping, adsorption, noncatalytic ozonation and catalytic ozonation experiments were carried out to explore the activity of RuO₂/ZrO₂-CeO₂ in a semi-batch reactor which was previously described in [13,14]. In these experiments, oxalic acid aqueous solution (5 mg·L⁻¹), DMP aqueous solution (5 mg·L⁻¹) and the natural water samples were used. Before the reaction, 1000 mL of solution was loaded into the reactor. If necessary, 2 g·L⁻¹ catalyst was also introduced into the reactor just before O₃ was fed in it. O₃ dosage was 116 mg·h⁻¹ and the flow rate of O₂/O₃ mixture was 400 mL·min⁻¹. During the reaction, the temperature of the reactor was kept at 15°C±0.5°C by the temperature-control system. The experiments were carried out for 180 min. At a pre-determined interval water samples were withdrawn from the reactor and the concentrations of DMP and ozone were analyzed.

2.2.2 Continuous experiments

Continuous experiments for the catalytic ozonation of oxalic acid were performed to investigate the stability of RuO₂/ZrO₂-CeO₂ in a dynamic reactor, which was developed from the semi-batch reactor by adding an influent pump. The hydraulic retention time was 60 min and the experiments were conducted for 48 h. The effluents of each continuous experiment were collected in a tank to analyze the concentration of metal, which was used to calculate the leached amounts from the catalyst into aqueous solution. For comparison, some continuous experiments were also conducted with Ru/AC or RuO₂/Al₂O₃. The preparation of Ru/AC and RuO₂/Al₂O₃ were specifically described in our previous works [13,14].

2.3 Analytical methods

2.3.1 Characterization of supports and catalysts

The Brunner–Emmet–Teller (BET) surface area was estimated at 77K by N₂ adsorption using an automated gas sorption analyzer (Quantachrome, Autosorb-1, USA). The analysis of X-ray powder diffraction (XRD) was carried out in a powder diffractometer (RIGAKU, D/max-III A, Japan) using Cu K α radiation ($\lambda = 1.5418\text{\AA}$). The actual ruthenium content of catalyst was determined by sequential X-ray fluorescence (XRF) spectrometry (Shimadzu, XRF-1700, Japan). The difference between the nominal and actual loading was less than 5%.

2.3.2 Analysis of ozone concentration, total organic carbon (TOC), UV₂₅₄ and metal concentration

The concentrations of ozone in aqueous solution were analyzed with indigo method [20]. Total organic carbon (TOC) was measured on a TOC analyzer (Shimadzu, TOC-Vwp, Japan). Water conductivity was determined using a conductivity meter (Rex, DDS-307, China). The analysis of UV₂₅₄ was carried out in a UV-Vis spectrophotometer (HACH, DR5000, USA). The concentrations of metal ion in aqueous solution were measured by inductively coupled plasma-mass spectrometry (ICP-MS) (Thermo Scientific, XSERIES 2, USA). Before the measurement, the water samples were filtered (0.45 μm) to remove suspended particles.

2.3.3 Analysis of oxalic acid and DMP

Oxalic acid concentration was determined by high performance liquid chromatography (HPLC) (Shimadzu, LC-10AD, Japan) with a UV-Vis detector (Shimadzu, SPD-10AV, Japan). A Spursil C18 column (150 mm long, 4.6 mm i.d) was used as fixed phase. The mobile phase was phosphoric acid solution with the concentration of 25 mmol·L⁻¹, pH value of 2.5 and flow rate of 1.0 mL·min⁻¹. The detection wavelength was 210 nm. DMP concentration was also analyzed by HPLC. A kromasil KR100-5 C18 column (250 mm long, 4.6 mm i.d) was used as fixed phase. The mobile phase was the mixture of methanol and water (v:v = 40:60) and its flow rate was 1.0 mL·min⁻¹. The detection wavelength was 254 nm.

2.3.4 Analysis of THMFP and HAAFP

According to the procedure described in Standard Methods of 5710 [21], the natural water samples were first buffered at pH = 7.0 and then chlorinated with an excess of free chlorine under standard conditions. After chlorination the water samples were stored at 25°C for 7 d to allow complete reaction. Trihalomethane formation potential (THMFP) and haloacetic acid formation potential (HAAFP) were analyzed according to the methods from 6232 B, 6251B, 5710, EPA 551 and EPA 552 [21,22].

The analysis of THMs was carried out using a liquid-liquid extraction-gas chromatographic method. A HP5890 II GC was used with an electron capture detector and an HP-5 capillary column (25 m \times 0.12 mm \times 0.133 μm). Good separations were achieved under the condition of 1 μL splitless injection, N₂ carrier gas with a linear velocity of 25 cm·s⁻¹, and a make-up gas flow rate of 30 mL·min⁻¹. The oven temperature program was set at 35°C for 5 min, rising 20°C min⁻¹ to 180°C, and a final hold time of 3 min. Total THMs concentration was achieved by simply summing individual components.

The analysis of HAAs was conducted with a modified liquid-liquid extraction-diazomethane methylation gas chromatographic method which was adopted from EPA 552 and APHA 6251B and optimized for the laboratory conditions. Excellent separations were also obtained under the condition of a split 1 μL injection, N_2 carrier gas with a linear velocity of $16 \text{ cm} \cdot \text{s}^{-1}$, and a make-up gas flow rate of $40 \text{ mL} \cdot \text{min}^{-1}$. The temperature program was: 40°C for 5 min, rising $20^\circ\text{C} \cdot \text{min}^{-1}$ to 130°C , rising $5^\circ\text{C} \cdot \text{min}^{-1}$ to 170°C , rising $25^\circ\text{C} \cdot \text{min}^{-1}$ to 240°C , and a final holding time of 3 min. Total HAAs (THAAs) concentrations were obtained by simple summation of individual components.

2.3.5 Quality control

For the analysis of THMs and HAAs, laboratory and field reagent blanks were analyzed and the results indicated that there was no interferences present in the reagents, apparatus, laboratory and field environment.

In the analysis of THMs, the separation of the THMs, internal standard (bromofluorobenzene), and surrogate (decafluorobiphenyl) was satisfactory. Seven aliquots of fortified reagent water were analyzed and the achieved detection limits was $0.04\text{--}0.10 \mu\text{g} \cdot \text{L}^{-1}$. Recoveries (79.3%–120%) and RSD (Relative Standard Deviation) for reproducibility (2.0%–11.2%) were satisfactory.

In the analysis of HAAs, the separation of the HAA esters, internal standard (trichloropropane), and surrogate (methyl 2,3-dibromopropionate) was also satisfactory. The analysis of seven aliquots of fortified reagent water shows the detection limits for HAA components ranged from 0.04 to $0.20 \mu\text{g} \cdot \text{L}^{-1}$. Recoveries (71.5%–125.4%) and RSD for reproducibility (2.1%–11.3%) met method requirements.

3 Results and discussion

3.1 BET surface area and XRD

The surface areas of powder $\text{ZrO}_2\text{-CeO}_2$ and $\text{RuO}_2/\text{ZrO}_2\text{-CeO}_2$ were 174 and $170 \text{ m}^2 \cdot \text{g}^{-1}$, respectively. Zr was poorly crystallized in both $\text{ZrO}_2\text{-CeO}_2$ and $\text{RuO}_2/\text{ZrO}_2\text{-CeO}_2$ probably due to the low calcination temperature (Fig. 1). Diffraction peaks as the attributive indicator of cubic CeO_2 ($2\theta = 28.57^\circ$, 33.10° , 47.53° and 56.38° , respectively) were observed in the XRD patterns for both $\text{ZrO}_2\text{-CeO}_2$ and $\text{RuO}_2/\text{ZrO}_2\text{-CeO}_2$. The XRD pattern of $\text{RuO}_2/\text{ZrO}_2\text{-CeO}_2$ indicates the characteristics of RuO_2 with three peaks ($2\theta = 28.12^\circ$, 35.18° and 54.44° , respectively). The intensities of the peaks were very weak mainly due to the low ruthenium loading amount.

3.2 Catalytic ozonation of oxalic acid in water

The experimental results for the catalytic ozonation of oxalic acid in water are shown in Fig. 2(a). In noncatalytic

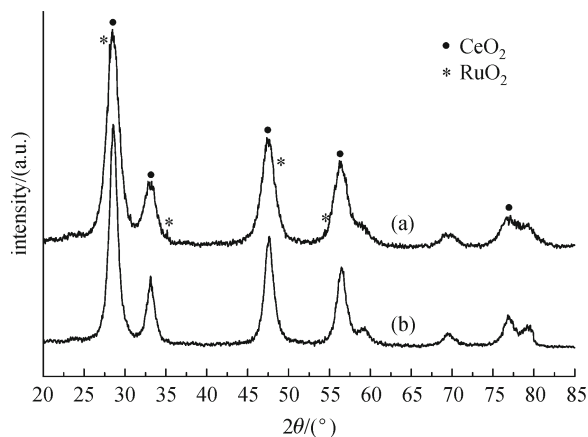


Fig. 1 XRD patterns of $\text{RuO}_2/\text{ZrO}_2\text{-CeO}_2$ (a) and $\text{ZrO}_2\text{-CeO}_2$ (b)

ozonation process, the oxalic acid removal was about 29% after 180 min, which is a little different from the results reported in the literatures [10,23]. The difference might be due to the different ratio of the initial oxalic acid concentration to ozone dosage between these studies. It is obvious that stripping had little effect on the removal of oxalic acid. The removal of oxalic acid in $\text{ZrO}_2\text{-CeO}_2$ catalyzed ozonation was a little higher than the sum of the oxalic acid removals in noncatalytic ozonation and $\text{ZrO}_2\text{-CeO}_2$ adsorption processes, indicating $\text{ZrO}_2\text{-CeO}_2$ exerts a little catalytic effect on the removal of oxalic acid. Catalytic ozonation with $\text{RuO}_2/\text{ZrO}_2\text{-CeO}_2$ led to about 69% oxalic acid conversion after 180 min reaction, indicating $\text{RuO}_2/\text{ZrO}_2\text{-CeO}_2$ was more active than $\text{ZrO}_2\text{-CeO}_2$.

Figure 2(b) shows the results obtained from the continuous experiments for the catalytic ozonation of oxalic acid with the different ruthenium catalysts. The catalytic activities for all the catalysts decreased gradually during the 48 h reaction. $\text{RuO}_2/\text{ZrO}_2\text{-CeO}_2$ possessed better stability than Ru/AC and $\text{RuO}_2/\text{Al}_2\text{O}_3$. Metal leaching would cause the loss of the activity of all the catalysts. The concentrations of ruthenium in the collected effluents for all the catalysts were about $0.0001 \text{ mg} \cdot \text{L}^{-1}$, which were higher than those observed in the catalytic ozonation of DMP in previous studies [13,14]. This was mainly due to the more acidic environment in the catalytic ozonation of oxalic acid. The leaching concentrations of zirconium and cerium from $\text{RuO}_2/\text{ZrO}_2\text{-CeO}_2$ were $0.0001 \text{ mg} \cdot \text{L}^{-1}$ and $0.004 \text{ mg} \cdot \text{L}^{-1}$, respectively, which were much lower than the leaching concentration of alumina from Al_2O_3 ($0.2 \text{ mg} \cdot \text{L}^{-1}$). This is probably why $\text{RuO}_2/\text{ZrO}_2\text{-CeO}_2$ was more stable than $\text{RuO}_2/\text{Al}_2\text{O}_3$. Ru/AC was less stable than $\text{RuO}_2/\text{ZrO}_2\text{-CeO}_2$ probably because of the oxidation of carbon by ozone [15].

As Ru is the active species for the catalyst of $\text{RuO}_2/\text{ZrO}_2\text{-CeO}_2$, it might be expected that catalyst activity would increase as the loading of Ru. So we evaluated the effect of Ru loading on catalytic activity and Fig. 3 shows

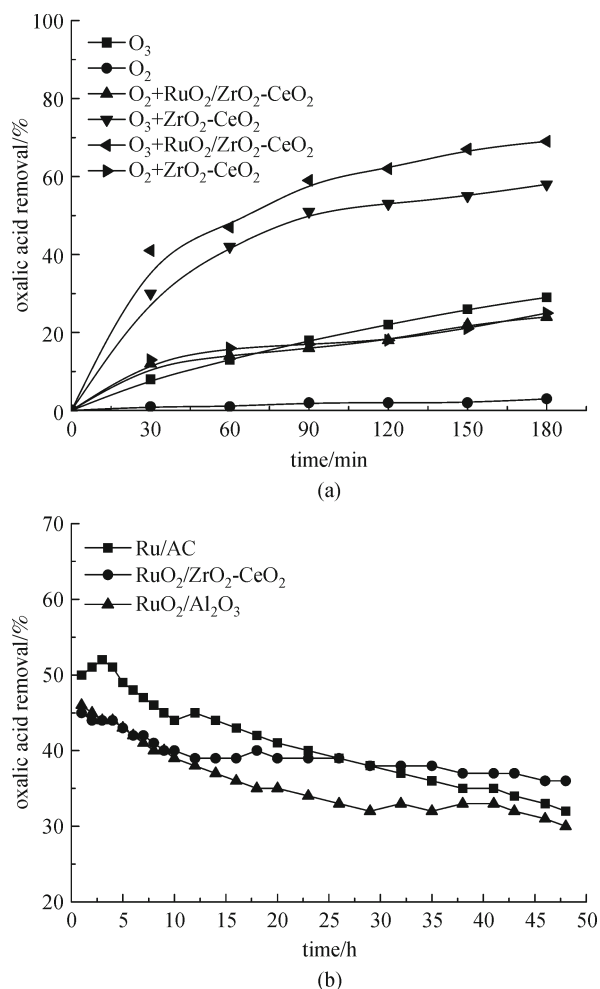


Fig. 2 Removals of oxalic acid in semi-batch (a) and dynamic (b) catalytic ozonation experiments

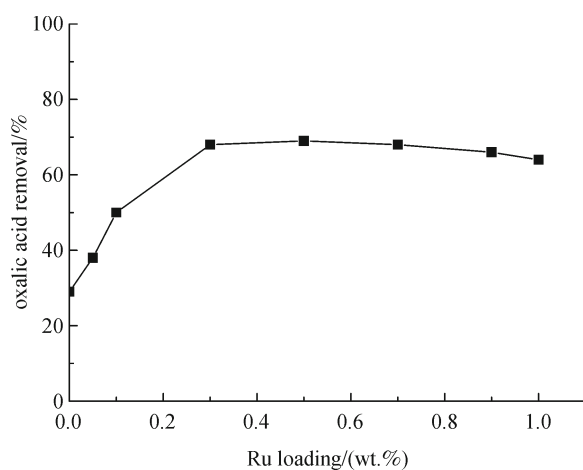


Fig. 3 Removal of oxalic acid in the catalytic ozonation with different Ru loading

the oxalic acid removals after 180 min reaction. With Ru loading ranging from 0 to 0.3 wt.%, the oxalic acid

removal significantly increased with Ru loading. When Ru loading is above 0.7 wt.%, the TOC removal begins declining. The decline may be occurred due to the content of Ru exceeding some threshold value. Ruthenium on the support of ZrO₂-CeO₂ formed larger crystals, leading to a decrease of the amount of active sites, followed by the activity decline. At the same time, the increase of Ru content would block the pores of RuO₂/ZrO₂-CeO₂ with its crystals, which resulted in the decrease of BET surface area and had a negative impact on the activity of the catalyst. So in this study we selected 0.5 wt.% as the optimal loading.

3.3 Catalytic ozonation of DMP in water

The degradation and mineralization of DMP are shown in Figs. 4(a) and 4(b) respectively. The effect of catalyst adsorption and stripping on the removal of DMP was negligible as the DMP removal in O₂ + RuO₂/ZrO₂-CeO₂ process was less than 10%. DMP was degraded fast in both

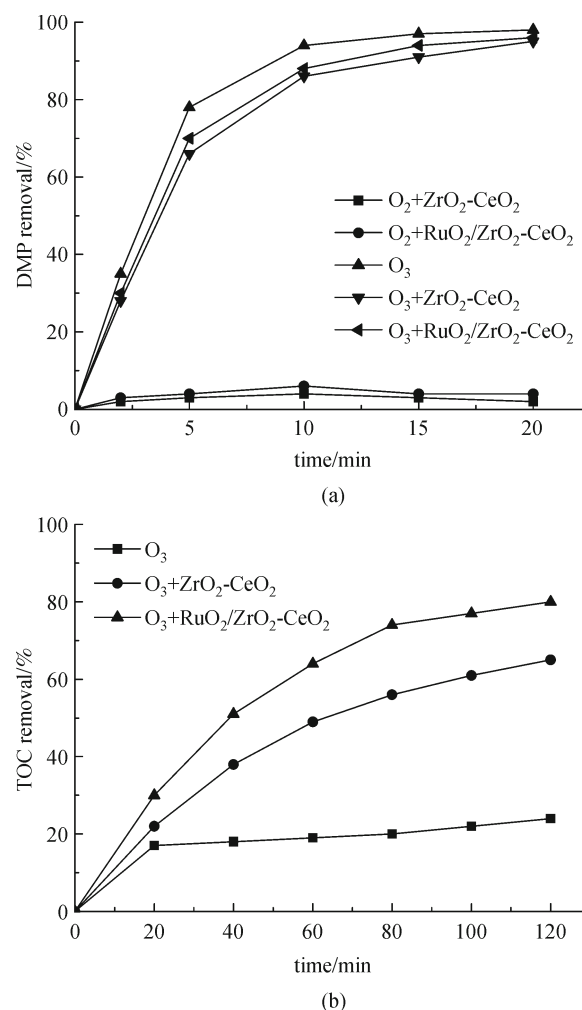


Fig. 4 Removals of DMP (a) and TOC (b) in catalytic ozonation of DMP in water

noncatalytic ozonation and catalytic ozonation processes, with more than 95% removal after 20 min reaction.

The TOC removal in noncatalytic ozonation process was only 24% after 120 min reaction. The low level of the mineralization of DMP in noncatalytic ozonation process was resulted from the accumulation of refractory intermediates (e.g., low molecular weight carboxylic acids) [1]. Both $\text{ZrO}_2\text{-CeO}_2$ and $\text{RuO}_2/\text{ZrO}_2\text{-CeO}_2$ significantly enhanced TOC removal in the catalytic ozonation of DMP in water. The TOC removal with $\text{RuO}_2/\text{ZrO}_2\text{-CeO}_2$ was 15% more than that with $\text{ZrO}_2\text{-CeO}_2$.

Significantly improved reaction rate and negligible adsorption are two essential criterions in evaluating catalytic activity [24]. In this study, the catalysts can absorb both DMP and the intermediates produced from the oxidation of DMP. The adsorption of DMP on the catalysts was proved to be negligible from the results of the adsorption experiments. To determine the contribution of adsorption to the total TOC removal, experiments were conducted in discontinuous mode according to the procedures described in our previous work [14]. The specific procedures are as the following: an aqueous solution of DMP ($5 \text{ mg} \cdot \text{L}^{-1}$) was treated with ozone for 20 min. Then the solution was degasified by the introduction of N_2 to remove dissolved ozone (Indigo method was used to follow the concentration of dissolved ozone). It took about 40 min to completely remove the dissolved ozone in water. The measurement showed that the TOC removal during the degasification was about 5% of the TOC removal obtained in 0–60 min reaction. After ozone was completely removed, $2 \text{ g} \cdot \text{L}^{-1}$ catalyst was added into the solution and O_2 was continuously pumped into the reactor for 100 min at the flow rate of $400 \text{ mL} \cdot \text{min}^{-1}$. At this condition the TOC removal was caused by the adsorption of catalysts.

The results of the above experiments are shown in Table 1. For 0–60 min, the TOC removal was resulted from ozonation. The TOC removal due to the adsorption of catalyst can be calculated by subtracting the contribution of ozonation from the overall TOC removal in the above discontinuous mode experiment. The contribution of catalysis was determined by subtracting the contributions of ozonation and catalyst adsorption from the overall TOC removal obtained after 120 min reaction in the experiments for the $\text{RuO}_2/\text{ZrO}_2\text{-CeO}_2$ catalyzed ozonation in the semi-batch reactor. The contribution of catalysis to the overall TOC removal was less than the contribution of adsorption (Table 1). So catalyst-enhanced TOC removal relative to

noncatalytic ozonation, with the value of 56%, does not mean $\text{RuO}_2/\text{ZrO}_2\text{-CeO}_2$ was very active because the contribution of catalysis to the overall TOC removal was 30%.

Based on the above observation, we can conclude that the effect of adsorption on TOC removal was obvious while the adsorption of DMP on the catalyst surface was negligible. This can be interpreted as the following: The reaction between O_3 and DMP was fast, and about 95% of DMP molecules were quickly oxidized into the intermediates after 20 min reaction in the $\text{RuO}_2/\text{ZrO}_2\text{-CeO}_2$ catalyzed ozonation. Most of intermediates are thought to be carboxylic acids [17]. As the reactions between ozone and carboxylic acids are slow [17], most of them would be removed by adsorption rather than by oxidation. So the effect of adsorption on TOC removal was obvious.

For organic compounds which react fast with ozone, their removal rates in noncatalytic ozonation differ little from those in catalytic ozonation. At this condition some authors measured their TOC removal rates in both noncatalytic ozonation and catalytic ozonation. Some of them concluded the catalyst was active for the mineralization of these organic compound when the TOC removal rate in catalytic ozonation was much larger than that in noncatalytic ozonation [13,25,26]. However, we think their method is flawed. They should carry out the measurement to determine the contribution of catalysis to the overall TOC removal.

In the study for the catalytic ozonation of an organic compound recalcitrant to ozonation, if the removal rate of this organic compound in catalytic ozonation process is much higher than that in noncatalytic ozonation and its adsorption on catalyst is negligible, we can conclude the used catalyst is active. At this condition we need not conduct the experiments to determine the contribution of catalysis to the overall TOC removal.

3.4 Catalytic ozonation of DBP precursors in natural water with $\text{RuO}_2/\text{ZrO}_2\text{-CeO}_2$

The common water quality parameters for the natural water samples are summarized in Table 2, and the MCAA, MBAA, DCAA, TCAA, BCAA, and BDCAA concentrations of the chlorinated natural water samples are shown in Table 3. Their HAAFPs were about $100 \mu\text{g} \cdot \text{L}^{-1}$, higher than the EPA guideline value ($60 \mu\text{g} \cdot \text{L}^{-1}$) [22,27]. TCAA, which possesses the highest carcinogenic risk among haloacetic acids, accounted for more than half of the

Table 1 Contributions of ozonation, adsorption and catalysis to the overall TOC removal

samples	total removal		ozonation		adsorption		catalysis	
	value/($\text{mg} \cdot \text{L}^{-1}$)	ratio/%	value/($\text{mg} \cdot \text{L}^{-1}$)	contribution/%	value/($\text{mg} \cdot \text{L}^{-1}$)	contribution/%	value/($\text{mg} \cdot \text{L}^{-1}$)	contribution/%
$\text{ZrO}_2\text{-CeO}_2$	2.01	65	0.62	31	1.01	50	0.39	19
$\text{RuO}_2/\text{ZrO}_2\text{-CeO}_2$	2.47	80	0.62	25	1.11	45	0.74	30

Table 2 Common water quality parameters for the natural water samples

No.	sampling site	TOC/(mg·L ⁻¹)		UV ₂₅₄		conductivity/(μs·cm ⁻¹)		pH	
		mean	std. dev.	mean	std. dev.	mean	std. dev.	mean	std. dev.
1	Qiaoxin Town	2.32	0.198	0.043	0.0073	339	28.5	7.7	0.42
2	Beishicao Town	2.25	0.157	0.043	0.0068	338	26.5	7.6	0.40
3	Xingshou Town	2.38	0.234	0.048	0.0039	329	25.8	8.1	0.35
4	Nanshao Town	2.50	0.224	0.046	0.0051	336	25.6	8.5	0.31
5	Machi Kou	2.47	0.225	0.048	0.0053	330	25.2	8.3	0.35
6	Yangfan Town	2.52	0.209	0.047	0.0046	327	24.2	8.2	0.31
7	Hotspring Town	2.45	0.228	0.048	0.0054	311	29.5	8.2	0.34
8	Blue-dragon Bridge	2.50	0.233	0.044	0.0049	308	25.9	8.1	0.28
9	Huoqiying Bridge	2.29	0.183	0.045	0.0050	310	29.5	7.7	0.40
10	Changchun Bridge	2.33	0.205	0.043	0.0036	301	23.6	7.4	0.24
11	Yuyuan Pond	3.20	0.278	0.064	0.0082	368	35.7	7.3	0.22

Table 3 Concentrations of haloacetic acids, HAAFPs and THMFPs of the natural water samples

samples	MCAA/(μg·L ⁻¹)		MBAA/(μg·L ⁻¹)		DCAA/(μg·L ⁻¹)		TCAA/(μg·L ⁻¹)		BCAA/(μg·L ⁻¹)		BDCAA/(μg·L ⁻¹)		HAAFP/(μg·L ⁻¹)	THMFP/(μg·L ⁻¹)
	mean	std. dev.	mean	std. dev.	mean	std. dev.	mean	std. dev.	mean	std. dev.	mean	std. dev.		
1	6.0	0.55	26.0	3.51	0.1	0.01	51.0	4.80	1.1	0.13	6.9	0.68	91.1	149.3
2	7.5	0.61	28.5	2.15	0.1	0.01	53.0	8.25	1.3	0.12	6.6	0.69	97.0	145.5
3	7.3	0.64	27.1	2.60	0.1	0.01	51.1	4.17	0.7	0.08	6.3	0.55	92.6	160.7
4	7.0	0.69	26.5	3.65	0.1	0.01	51.8	4.22	0.6	0.08	6.2	0.51	92.2	156.4
5	7.5	0.63	26.7	1.75	0.2	0.01	52.3	4.48	0.7	0.08	6.3	0.57	93.7	163.7
6	8.3	0.67	28.0	5.00	0.1	0.02	53.7	4.30	0.8	0.10	6.4	0.59	97.3	163.0
7	7.2	0.68	27.0	2.83	0.4	0.05	58.9	7.40	1.5	0.14	6.3	0.67	101.3	160.2
8	6.8	0.58	26.5	2.34	0.3	0.03	56.3	6.12	1.6	0.23	6.3	0.63	97.8	165.8
9	6.3	0.54	25.0	3.83	0.1	0.02	55.4	5.68	1.5	0.20	6.1	0.51	94.4	152.4
10	6.8	0.68	25.3	2.74	0.3	0.02	57.1	5.80	1.7	0.14	6.1	0.55	97.3	150.1
11	27.0	3.56	30.2	2.97	0.1	0.01	76.1	6.32	2.0	0.16	7.1	0.64	142.5	220.0

HAAFPs. The chlorinated water may cause high carcinogenic risk and the source water of Beijing City should be pretreated to remove DBP precursors before chlorination.

Figure 5 shows the removals of the DBP precursors by the pretreatment of catalyst adsorption, noncatalytic ozonation and RuO₂/ZrO₂-CeO₂ catalyzed ozonation processes. Catalyst adsorption could hardly lower the HAAFPs of the water samples below the EPA guideline value. Though ozonation has been shown to be effective for destroying the DBP precursors [28], in this study preozonation could not lower the HAAFPs of some water samples below the guideline value. It was reported that the effects of ozonation on DBP precursor destruction were quite site-specific and unpredictable. The nature of the organic material is one of the important variables determining ozone's effect [29]. Since natural organic matter (NOM) is a broad mix of molecules with different

structures, it is not surprising that some types of NOM show a different trend in DBP formation with oxidation.

When the water samples were pretreated by the RuO₂/ZrO₂-CeO₂ + O₃ process, the reductions of their HAAFPs, TCCA formation potential (TCCAFP) and THMFPs were 38%–57%, 67%–78% and 50%–64%, respectively. The HAAFPs could decrease below the EPA guideline value. RuO₂/ZrO₂-CeO₂ was active in catalytic ozonation for the oxidation of DBP precursors. However, RuO₂/ZrO₂-CeO₂ did not significantly enhance the reductions of THMFPs relative to noncatalytic ozonation. This is perhaps because ozone reacts fast with the THMs precursors, which can be inferred from the fact that the reductions of the THMFPs of the water samples in the noncatalytic ozonation process were high (Fig. 5(c)). In our previous work [13], we also found that Ru/AC is active for the reduction of HAAFPs but inactive for THMFPs.

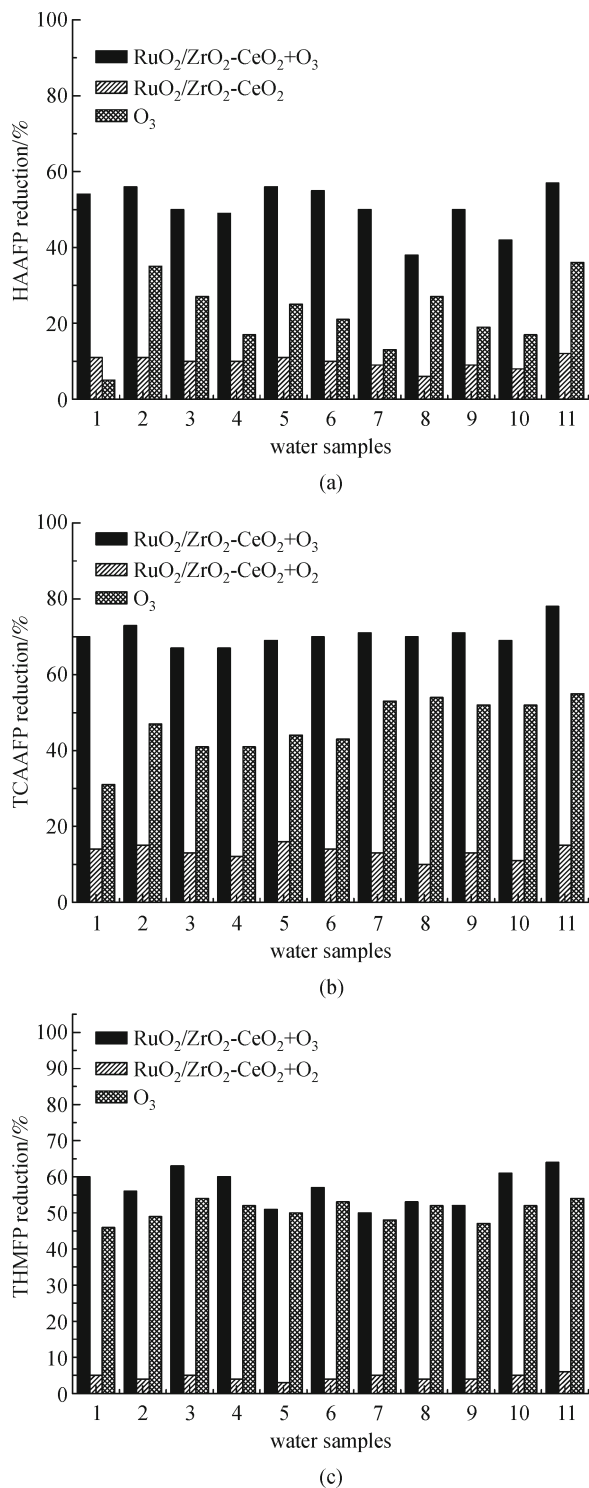


Fig. 5 Reductions of HAAFP (a), TCAAFF (b) and THMFP (c) in adsorption, noncatalytic ozonation and catalytic ozonation processes

Because of its selectivity for olefinic bonds, molecular ozone appears to be more effective than less selective hydroxyl radicals for the removal of organic DBP precursors [28]. H₂O₂/O₃ process was reported to be less

effective for precursor destruction than simple ozonation [30]. However, in this work catalytic ozonation is more effective for the removal of DBP precursors than noncatalytic ozonation. Jacangelo et al. [29] reported that the key variables determining ozone's effect include dose, pH, and alkalinity. We thought the high ozone dosage in this study is the reason why catalytic ozonation are more active than noncatalytic ozonation for DBP precursor destruction. The pH of the natural water samples is about 7.0, and at this pH only one part of the ozone reacts directly with NOM. The other part of ozone may decompose into some reactive secondary oxidants. As the concentration of DBP precursors in the natural water samples was low, the direct reaction between ozone and NOM was enough to oxidize the DBP precursors containing olefinic bonds. The reactive secondary oxidants such as OH· produced from the decomposition of ozone can oxidize the DBP precursors without olefinic bonds because of its non-selective oxidation effect. Thus in this study catalytic ozonation process is more effective for the removal of DBP precursors than noncatalytic ozonation.

3.5 Proposed reaction mechanism for catalytic ozonation with RuO₂/ZrO₂-CeO₂

Metal oxide was found to catalyze the decomposition of oxalic acid by the transformation of ozone into HO· radicals which are more active than ozone in the liquid phase [12]. In this study we proposed the formation of Ru (III) species promotes the decomposition of O₃ into HO· radicals by redox reactions on the catalyst surface involving the pair Ru(III)/Ru(IV). We thought the load of ruthenium on CeO₂ may help this process as it was reported that Ru–O–Ce bonds in the well-dispersed Ru species are highly fragile and play an important role for the catalytic activity of ruthenium supported catalysts [31]. ZrO₂ incorporation makes ZrO₂-CeO₂ possessing a higher reduction efficiency of redox couple Ce⁴⁺/Ce³⁺ than CeO₂ [32]. Thus in this study, both Ce and Zr species in the catalysts can enhance the catalytic activity of ruthenium species.

4 Conclusions

RuO₂/ZrO₂-CeO₂ was prepared and its performance in catalytic ozonation for the treatment of oxalic acid, DMP and DBP precursors in water was studied. RuO₂/ZrO₂-CeO₂ was active for the removal of oxalic acid in water. During the long time reaction it showed higher stability than RuO₂/Al₂O₃ and Ru/AC. RuO₂/ZrO₂-CeO₂ significantly improved TOC removal in the catalytic ozonation of DMP in water. However, this doesn't mean it was very active as the contribution of catalysis to the overall TOC removal was less than that of catalyst adsorption. RuO₂/ZrO₂-CeO₂ was active for the reductions of HAAFPs but

inactive for the reductions of THMFPs of the natural water samples. As RuO₂/ZrO₂-CeO₂ prepared in this study is active and stable, it might have a great potential to apply in the field of catalytic ozonation.

Acknowledgements This work was supported by the National Natural Science Foundation of China (Grant No. 20907072).

Supplementary material is available in the online version of this article at <http://dx.doi.org/10.1007/s11783-014-0706-5> and is accessible for authorized users.

References

- Huang R H, Yan H H, Li L S, Deng D Y, Shu Y H, Zhang Q Y. Catalytic activity of Fe/SBA-15 for ozonation of dimethyl phthalate in aqueous solution. *Applied Catalysis B: Environmental*, 2011, 106 (1): 264–271
- Li D, Qu J. The progress of catalytic technologies in water purification: a review. *Journal of Environmental Sciences-China*, 2009, 21(6): 713–719
- Chang C C, Chiu C Y, Chang C Y, Chang C F, Chen Y H, Ji D R, Yu Y H, Chiang P C. Combined photolysis and catalytic ozonation of dimethyl phthalate in a high-gravity rotating packed bed. *Journal of Hazardous Materials*, 2009, 161(1): 287–293
- Zhou H, Zhang X J, Wang Z S. Occurrence of haloacetic acids in drinking water in certain cities of China. *Biomedical and Environmental Sciences*, 2004, 17(3): 299–308
- Li S, Zhang X J, Liu W J, Cao L L, Wang Z S. Formation and evolution of haloacetic acids in drinking water of Beijing City. *Journal of Environmental Science and Health, Part A: Toxic/Hazardous Substances and Environmental Engineering*, 2001, 36 (4): 475–481
- Chen C, Zhang X J, Zhu L X, Liu J, He W J, Han H D. Disinfection by-products and their precursors in a water treatment plant in North China: Seasonal changes and fraction analysis. *Science of the Total Environment*, 2008, 397(1–3): 140–147
- Legube B, Karpel N V L. Catalytic ozonation: a promising advanced oxidation technology for water treatment. *Catalysis Today*, 1999, 53 (1): 61–72
- Chen Y H, Shang N C, Hsieh D C. Decomposition of dimethyl phthalate in an aqueous solution by ozonation with high silica zeolites and UV radiation. *Journal of Hazardous Materials*, 2008, 157(2–3): 260–268
- Álvarez P M, Beltrán F J, Pocostales J P, Masa F J. Preparation and structural characterization of Co/Al₂O₃ catalysts for the ozonation of pyruvic acid. *Applied Catalysis B: Environmental*, 2007, 72(3–4): 322–330
- Beltran F J, Rivas F J, Ramon M E A. TiO₂/Al₂O₃ catalyst to improve the ozonation of oxalic acid in water. *Applied Catalysis B: Environmental*, 2004, 47(2): 101–109
- Qu J H, Li H Y, Liu H J, He H. Ozonation of alachlor catalyzed by Cu/Al₂O₃ in water. *Catalysis Today*, 2004, 90(3–4): 291–296
- Faria P C C, Órfão J J M, Pereira M F. A novel ceria-activated carbon composite for the catalytic ozonation of carboxylic acids. *Catalysis Communication*, 2008, 9(s 11–12): 2121–2126
- Wang J, Zhou Y, Zhu W, He X. Catalytic ozonation of dimethyl phthalate and chlorination disinfection by-product precursors over Ru/AC. *Journal of Hazardous Materials*, 2009, 166(1): 502–507
- Zhou Y, Zhu W, Liu F, Wang J, Yang S. Catalytic activity of Ru/Al₂O₃ for ozonation of dimethyl phthalate in aqueous solution. *Chemosphere*, 2007, 66(1): 145–150
- Alvárez P M, Beltrán F J, Masa F J, Pocostales J P. A comparison between catalytic ozonation and activated carbon adsorption/ozone-regeneration processes for wastewater treatment. *Applied Catalysis B: Environmental*, 2009, 92(3–4): 393–400
- Wang J B, Zhu W P, Yang S X, Wang W, Zhou Y R. Catalytic wet air oxidation of phenol with pelletized ruthenium catalyst. *Applied Catalysis B: Environmental*, 2008, 78(1–2): 30–37
- Imamura S, Fukuda I, Ishida S. Wet oxidation catalyzed by ruthenium supported on cerium (IV) oxides. *Industrial & Engineering Chemistry Research*, 1988, 27(4): 718–721
- Gallezot P, Chaumet S, Perrard A, Isnard P. Catalytic wet air oxidation of acetic acid on carbon-supported ruthenium catalysts. *Journal of Catalysis*, 1997, 168(1): 104–109
- Beltran F J. *Ozonation Reaction Kinetics for Water and Wastewater Systems*. Boca Raton: CRC Press, 2004
- Bader H, Hoingé J. Determination of ozone in water by the indigo method. *Water Research*, 1981, 15(4): 449–456
- Clescerl L S, Greenberg A E, Eaton A D. *Standard Methods for the Examination of Water and Wastewater*. Washington, DC: American Public Health Association, 2012
- Buchanan W, Roddick F, Porter N. Removal of VUV pre-treated natural organic matter by biologically activated carbon columns. *Water Research*, 2008, 42(13): 3335–3342
- Andreozzi R, Insola A, Caprio V, D'Amore M G. The kinetics of Mn(II)-catalysed ozonation of oxalic acid in aqueous solution. *Water Research*, 1992, 26(7): 917–921
- Rivera-Utrilla J, Sanchez-Polo M. Ozonation of 1,3,6-naphthalene-trisulphonic acid catalysed by activated carbon in aqueous phase. *Applied Catalysis B: Environmental*, 2002, 39(4): 319–329
- Xing S, Hu C, Qu J, He H, Yang M. Characterization and reactivity of MnO(x) supported on mesoporous zirconia for herbicide 2,4-D mineralization with ozone. *Environmental Science & Technology*, 2008, 42(9): 3363–3368
- Orge C A, Orfao J J M, Pereira M F R, Farias A M D, Netob R C R, Fragab M A. Ozonation of model organic compounds catalysed by nanostructured cerium oxides. *Applied Catalysis B: Environmental*, 2011, 103(1–2): 190–199
- Buchanan W, Roddick F, Porter N. Formation of hazardous by-products resulting from the irradiation of natural organic matter: Comparison between UV and VUV irradiation. *Chemosphere*, 2006, 63(7): 1130–1141
- Edzwald J K. *Water Quality & Treatment: A Handbook on Drinking Water*. New York: McGraw Hill, 2011
- Jacangelo J G, Patania N L, Reagan K M, Aieta E M, Krasner S W, McGuire M J. Ozonation: assessing its role in the formation and control of disinfection by-products. *Journal-American Water Works Association*, 1989, 81(8): 74–84
- Kleiser G, Frimmel F H. Removal of precursors for disinfection by-products (Dbps)—differences between ozone- and OH-radical-

- induced oxidation. *Science of the Total Environment*, 2000, 256(1): 1–9
31. Hosokawa S, Kanai H, Utani K, Taniguchi Y, Saito Y, Imamura S. State of Ru on CeO₂ and its catalytic activity in the wet oxidation of acetic acid. *Applied Catalysis B: Environmental*, 2003, 45(3): 181–187
32. Vidal H, Kašpara J, Pijolat M, Colomb G, Bernal S, Cordon A, Perrichon V, Fally F. Redox behavior of CeO₂–ZrO₂ mixed oxides I. Influence of redox treatments on high surface area catalysts. *Applied Catalysis B: Environmental*, 2000, 27(1): 49–63